

Article

Impact of Dense Water Formation on the Transfer of Particles and Trace Metals from the Coast to the Deep in the Northwestern Mediterranean

X. Durrieu de Madron ^{1,*}, D. Aubert ¹ , B. Charrière ¹ , S. Kunesch ¹, C. Menniti ¹, O. Radakovitch ² and J. Sola ¹

¹ Centre de Formation et de Recherche sur les Environnements Méditerranéens, UMR 5110, CNRS-Université de Perpignan Via Domitia, 52 Avenue Paul Alduy, 66860 Perpignan, France

² Institut de Radioprotection et de Sécurité Nucléaire, PSE/SRTE/LRTA, BP 3, 13115 Saint-Paul-Lez-Durance, France

* Correspondence: demadron@univ-perp.fr

Abstract: This study aimed to describe the interannual variability of dense shelf water cascading and open ocean convection in the Gulf of Lions (NW Mediterranean) based on long-term temperature and current records and its impact on particle fluxes and associated metals. These observations highlight the predominant role of the rare intense events of dense shelf water cascading (1999/2000, 2005/2006, 2012/2013) in the basinward export of particles, which are mainly brought by rivers. Measurements of particulate trace metals in 2012 indicate that the monitored intense cascading event may be responsible for a significant fraction (~15%) of the annual input to the shelf. To this first process is added the effect of somehow more recurrent deep convection events (2005, 2009–2013) that remobilize the deep sediments, receptacle of coastal inputs, and disperse them rapidly at the scale of the northern Mediterranean basin, and gradually over the entire western basin. Coastal and oceanic dense water formations are key physical processes in the Mediterranean margins, whose reduction in intensity and recurrence has already been observed and also anticipate in climate scenarios that will likely change the dispersion pathways of chemical particles in this region.

Keywords: dense water formation; cascading; convection; Mediterranean; particulate flux; metals; long term changes



Citation: Durrieu de Madron, X.; Aubert, D.; Charrière, B.; Kunesch, S.; Menniti, C.; Radakovitch, O.; Sola, J. Impact of Dense Water Formation on the Transfer of Particles and Trace Metals from the Coast to the Deep in the Northwestern Mediterranean. *Water* **2023**, *15*, 301. <https://doi.org/10.3390/w15020301>

Academic Editor: Bommanna Krishnappan

Received: 22 November 2022

Revised: 6 January 2023

Accepted: 8 January 2023

Published: 11 January 2023



Copyright: © 2023 by the authors. Licensee MDPI, Basel, Switzerland. This article is an open access article distributed under the terms and conditions of the Creative Commons Attribution (CC BY) license (<https://creativecommons.org/licenses/by/4.0/>).

1. Introduction

Coastal marine environments are key repository environments for natural or anthropogenic inputs of particulate material, particularly metals. These inputs, mainly of fluvial and atmospheric origin, can be stored in coastal sediments (e.g., [1–5]), reworked, and partly exported to the open sea by multiple hydrodynamic processes [6–10]. Because of the reduced solubility of metals in the common pH and redox conditions of oceanic waters, the dominant part of trace metals is transported in association with particulates (in the following: particulate trace metals, PTM).

The Gulf of Lions, in the northwestern Mediterranean, is highly interesting for the study of PTM fluxes from land to sea, as it is abundantly supplied by both river discharges and atmospheric deposition, and presents some shelf-slope exchange mechanisms that are very effective in exporting shelf water toward the open sea and the deep part of the basin [11]. The synthesis of [12] clearly describes the complexity of the intense and variable hydrodynamic phenomena that simultaneously take part in this region. Among these phenomena, the formation of dense water, produced in winter by heat loss associated with northern continental winds (Tramontane and Mistral), is central. The coastal waters are cooled, homogenized, and densified. They propagate mainly along the western coast of the Gulf of Lions, in a cyclonic manner driven by wind-induced winds, and are exported from the shelf at the level of its SW end incised by the Lacaze-Duthiers and Cap de Creus

Canyons. There, they cascade down the slope, sometimes to more than 2000 m for the most intense events. This dense shelf water cascading process is called simply cascading hereafter. In the basin, open-ocean convection involves a progressive deepening of the upper oceanic mixed layer, which first reaches the intermediate water and eventually extends to the bottom, if the atmospheric forcing is sufficiently intense. This process is typically composed of three phases: the preconditioning phase, the intense mixing phase, and the restratification-spreading phase [13]. During the fall and early winter preconditioning, northern winds strengthen the cyclonic circulation in the Gulf of Lions, which traps and upwells the surface and intermediate waters in the center of the basin. During the intense winter mixing phase, the high atmospheric heat loss makes the surface water dense enough to sink to depth and form a homogeneous convective patch of dense water. Finally, during the restratification-spreading phase, the patch of dense water sinks and spreads out at depth while the lighter surrounding waters reinvest the area.

Previous studies have already provided insights into the distribution and enrichment of PTM in recent surface sediments of the Gulf of Lions [14–16] on the potential contributions of the Rhône River [17,18] and other coastal rivers [16,19] to the marine PTM stocks as well as on their further offshore transport to deep-sea environments via the submarine canyons [16,20,21].

Long-term monitoring of particle flux and currents is being conducted in various canyons incising the continental slope. This has shown an increased shelf export of particulate matter in the western part of the gulf, and that fall and winter eastern storms and winter cascades of dense shelf water are responsible for increased transfer through canyons toward the upper slope [22,23]. Only rare and severe cascading events, observed in 1999, 2005, 2006, and 2012, could export of shelf particulate matter directly to the deep slope and basin [24–26].

Monitoring of particle fluxes and currents was also carried out in the central part of the basin of the Gulf of Lions (Figure 1). Observations have revealed the importance of deep-water formation by convection on the near-bottom particle fluxes, which are primarily composed of resuspended deep sediment [27,28]. The effect of bottom-reaching convection to the particle fluxes in the basin adds up to the impact of deep dense shelf water cascading, which supplies a significant amount of sediment from the shelf and slope [29,30].

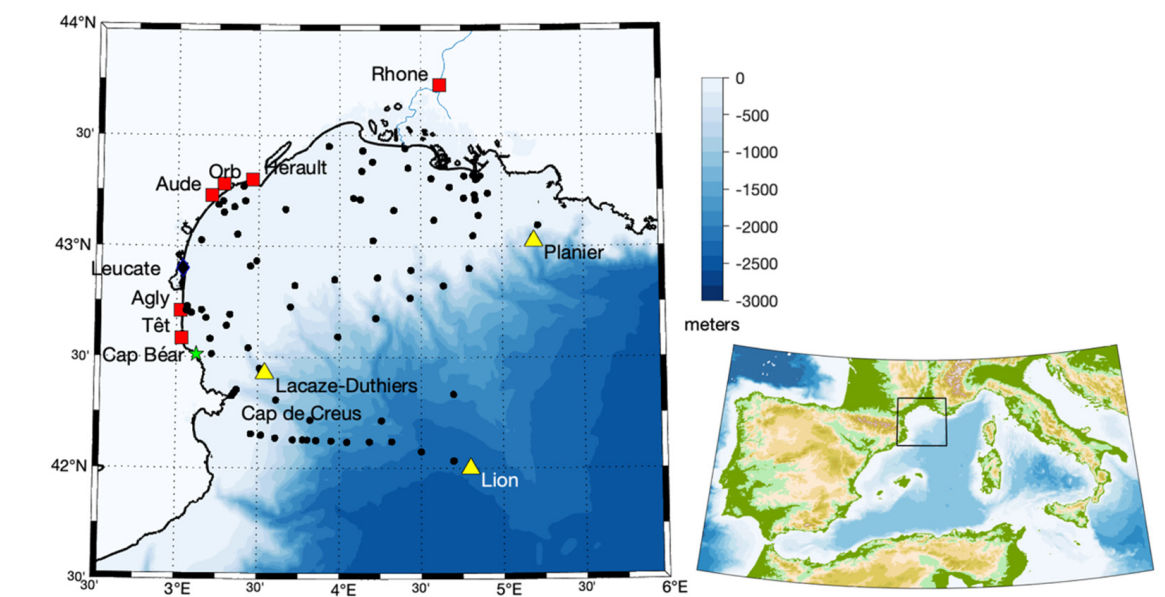


Figure 1. Map of the study area with the locations of the measurement sites (sampling stations in rivers—red squares; atmospheric station—green star, oceanic mooring lines with sediment traps in canyons and in the basin—yellow triangles, sediment cores on the shelf and in the basin—black dots).

During the winter of 2012, a major event of dense shelf water cascading and bottom-reaching convection took place in the Gulf of Lions. The origin, timing, and consequence in terms of the formation and spread of newly formed deep water throughout the NW Mediterranean basin is described in [26].

The implementation of numerous moorings equipped with sediment traps during this event allowed us to assess, for the first time, the role of this type of event on the transfer of metals between the shelf and the slope as well as in the basin and to infer their interactions. For this, the discussion will focus on the study of (a) the temporal variability of mass fluxes (rivers, atmosphere, slope, basin) over the period 2010–2017; (b) the key PTM concentrations in the different matrices (rivers, atmosphere, suspended particles, sediments) during the year 2012; and (c) the evaluation of the PTM fluxes transported during these events.

2. Materials and Methods

2.1. Field Measurements

Field data to estimate atmospheric, riverine, or oceanic particulate fluxes were acquired over the period 2010–2017. Trace metal analyses were limited to samples over the year 2012, which encompasses the main dense water formation event observed between January 2010 and December 2017.

2.1.1. Atmospheric Deposition

Saharan dust is a major source of atmospheric particulate inputs to the Mediterranean Sea [31,32]. Atmospheric depositions were measured at Cap Béar at the southwestern end of the Gulf of Lions (Figure 1). Dry and wet atmospheric depositions were collected separately with a 1000 ARS device (MTX-Italia SPA, Modane, Italy). This sampler performs sampling at 1.50 m above the ground and consists of two polyethylene cylinders with a surface of 0.064 m² and a removable lid, whose position was electronically controlled by a precipitation sensor. Dry and wet deposition was collected every 15 days. The bucket containing wet deposition was sealed, placed in a clean bag, and brought back to the laboratory for processing.

2.1.2. River Discharges

More than ten rivers drain the area adjacent to the Gulf of Lions. Ignoring the smallest ones, these are the Tech, Têt, Agly, Aude, Orb, Hérault, and Rhône Rivers (Figure 1). The freshwater and particulate matter inputs are dominated by the Rhône River, in the northeastern part of the area, which delivers ~80% of the total discharge [33]. The water flow data for each river were retrieved from the 'Banque Hydro' database administered by the French Ministry of the Environment. Solid discharges were then derived from the water discharges using the rating curve derived by [33]. The six rivers above-mentioned were sampled on a monthly basis. Water samples were collected for PTMs from the bridge closest to their mouth using a bucket and polyethylene bottles previously washed three times with 10% HCl-ultrapure and rinsed with MilliQ ultrapure water. These data are available for the period September 2011–September 2012.

2.1.3. Hydrology and Particulate Fluxes

Three mooring lines located on the continental slope and in the basin of the Gulf of Lions were used to record the temperature, current, and particle flux variability. The shallowest mooring lines were located at about 1000 m depth in the Planier Canyon (Figure 1) and Lacaze-Duthiers Canyon (Figure 1). These moorings were equipped with two pairs of traps and current meters, one near the bottom (~30 m above the bottom), and the other at mid-depth (~500 m above the bottom). A third deep line, equipped with a sediment trap and a current meter at ~30 m above the bottom, was located at a 2400 m depth in the basin at the center of the convection zone (LION site, Figure 1).

All traps were PPS3 Technicap (La Turbie, France) sediment traps that were cylindrical in shape with a 0.4 m opening diameter (2.5 height/diameter aspect ratio for the cylindrical part) and equipped with 12 sampling cups [34]. These were coupled with current meters (Nortek Aquadopp, Rud, Norway) located 2 m below the traps. The trap sampling interval was set at 14 days or 1 month. Current meters recorded pressure, temperature, current speed, and direction at 1 h intervals. These records are available for the period October 1993–June 2022 [35].

2.1.4. Sediment Data

A collection of surface sediment samples (Figure 1) was collected on the shelf during the REMORA3 cruise [36] in October 2002, the DEEP4 cruise [37] in October 2009, and the CASCADE cruise [38] in March 2011. Sediments cores were collected using a multiple corer, allowing for the sampling of undisturbed surface sediment. Surface sediment (0–1 cm) samples were collected placed in polyethylene plastic bags, stored in the dark at $-20\text{ }^{\circ}\text{C}$, freeze-dried, and homogenized prior to analysis.

2.2. Laboratory Analysis

2.2.1. Sediment Trap Samples

A detailed description of the PPS3 sediment trap and the sample processing used during this experiment can be found in [34], and the main steps are therefore only summarized here. The trap sampling cups were filled before deployment with a buffered 5% (*v/v*) formaldehyde solution in $0.45\text{ }\mu\text{m}$ filtered seawater. This poisoning solution limits the degradation of trapped particles and prevents the mechanical disruption of swimming organisms ('swimmers') that occasionally enter the traps during sampling. After recovery, the cups were stored in the dark at $2\text{--}4\text{ }^{\circ}\text{C}$ until they could be processed in the laboratory, within a maximum delay of a few months. After decantation of the supernatant, particles were wet sieved through a 1 mm nylon mesh to retain the largest swimmers. Smaller ones were removed under a dissecting microscope using fine-tipped tweezers. The original samples were then precisely divided into subsamples for subsequent analyses using a rotary splitting method. Sample dry weights, from which the total mass fluxes were calculated, were determined on four subsamples filtered onto $0.45\text{ }\mu\text{m}$ Merck Millipore (Burlington, VT, USA) cellulose acetate filters, rinsed with distilled water to remove salts, and dried at $40\text{ }^{\circ}\text{C}$ for 24 h.

2.2.2. Particulate Trace Metals

River, atmospheric, trap, and sediment samples were filtered on decontaminated cellulose acetate filters (Sartorius (Göttingen, Germany) SM 11106, 47 mm diameter, $0.45\text{ }\mu\text{m}$ porosity). The filters were dried under a laminar flow hood and stored in Petri dishes. These were kept in a desiccator until mineralization. Mineralization of the dried material was performed in Teflon beakers with successive mixtures of high quality (trace metals grade) nitric and hydrofluoric acids ($\text{HNO}_3\text{--HF}$) and nitric acid and oxygen peroxide ($\text{HNO}_3\text{--H}_2\text{O}_2$). Major and trace element concentrations were measured by inductively coupled plasma mass spectrometry (ICP-MS). The reference material was mineralized and analyzed under the same conditions as the samples and provided suitable recoveries (errors $< 5\%$ for Al, Co, Ni and Pb; recovery of Fe was 99%, recoveries of Cr, Cu, Zn, and Cd ranged from 90% to 96%, 111% to 122%, 109% to 146%, and 86% to 95%, respectively). Analytical blanks did not reveal any significant sign of contamination (contribution $< 0.5\%$ for Al, Fe, Cr, Co, Ni, Zn, Cs, and Pb, $< 1.5\%$ for Cu, and $< 3\%$ for Cd). A normalization of the elemental contents with respect to a reference element such as Al was applied to compensate for the grain size and mineralogical effects of the particulate material. The authors in [39] showed that the Al contents adequately reflected the grain size variability of the deep sediments in the study area.

Particulate organic carbon (POC) contents in the PTM samples were measured on an elemental analyzer after separate filtration on pre-weighted and preheated Whatman (Little

Chalfont, UK) GFF filters (47 mm in diameter and $<0.7 \mu\text{m}$ pore size) and the removal of inorganic carbon by repeated additions of 25% HCl. Filtration on GFF filters was used for the determination of the representative suspended particulate matter (SPM) concentrations in all samples, which were analyzed for PTM.

2.2.3. Current Meter

Temperatures were corrected and validated by comparison with measurements obtained by a Conductivity, Temperature, Depth (CTD) probe before the recovery of the mooring lines. Acoustic echo intensity records were used as a proxy for the concentration of suspended particulate matter concentration. The current meter acoustic frequency at 2 MHz leads to a peak sensitivity for particles around $250 \mu\text{m}$ [40].

3. Results

3.1. 2010–2017 Time Series of Temperature, Wave, Current, and Acoustic Backscatter

The 8-year records (2010–2017) of temperature and current, measured at mid-water (500 m) and near-bottom (1000 m) in the Planier and Lacaze-Duthiers Canyons as well as near-bottom at 2400 m in the deep basin, are shown in Figures 2 and 3. Records of significant wave height at the coast as well as the near-bottom backscatter index in the Lacaze-Duthiers Canyon and in the basin are shown in Figure 4.

Temperature records at 500 m depth in both canyons (Figure 2a) clearly showed a seasonal signal, with winter cooling and increasing currents up to 20 cm/s (Figure 3a). Temperatures at this depth have shown a significant upward trend as well as a weakening of winter fluctuations since 2014 (Figure 2a).

At the 1000 m depth near the bottom, the temperature (Figure 2b) and current (Figure 3b) showed moderate fluctuations in Planier Canyon, while intense peaks appeared in the Lacaze-Duthiers Canyon, especially during the winter of 2012, and to a lesser extent during the winter of 2013. These peaks are the signatures of extreme events of cold, dense coastal water that cascade down the canyon in the southwestern part of the Gulf of Lions margin.

Records near the bottom of the basin showed a period between 2010 and 2013 with temperature jumps (Figure 2c) and increased currents (Figure 3c) in late winter and spring. Afterward, this seasonal variability declined for currents and was almost absent for temperature. Temperature increases of a few hundredths of a degree are the signature of deep convection events that reach the bottom after mixing with the warmer and saltier intermediate waters. The temperature drop observed in 2012, following the deep convection event, resulted from the arrival of very dense (colder and less saline) bottom water from the continental shelf. The increase in currents (Figure 3c) observed after the deep convection resulted from the spread of newly formed deep water during the spring relaxation period.

The significant wave height (Figure 4a) is an indicator of short E–SE storms that cause strong currents that resuspend fine sediments from the inner shelf [41,42] and transport them to the sub-western end of the Gulf of Lions, up to the head of the Lacaze-Duthiers Canyon as well as that of the Cap de Creus Canyon, which adjoins it further south (Figure 1). These storms occur mainly in autumn and winter. The most notable storm periods were autumn 2010/winter 2011, autumn 2011, autumn 2012/winter 2013, and autumn 2016/winter 2017. In the deep part of the Lacaze-Duthiers Canyon (Figure 4b), notable increases in the backscatter index, and thus suspended particulate material, were visible for the dense coastal water events of winter 2012 and 2013. In the basin (Figure 4c), the backscatter signal showed spring increases between 2010 and 2013 that corresponded to intensified bottom currents and reflect the resuspension of deep sediments. No notable signals were recorded thereafter in the canyon or basin.

The interactions between convection and cascading and their effects on sediment dynamics have been described in detail by [26–28].

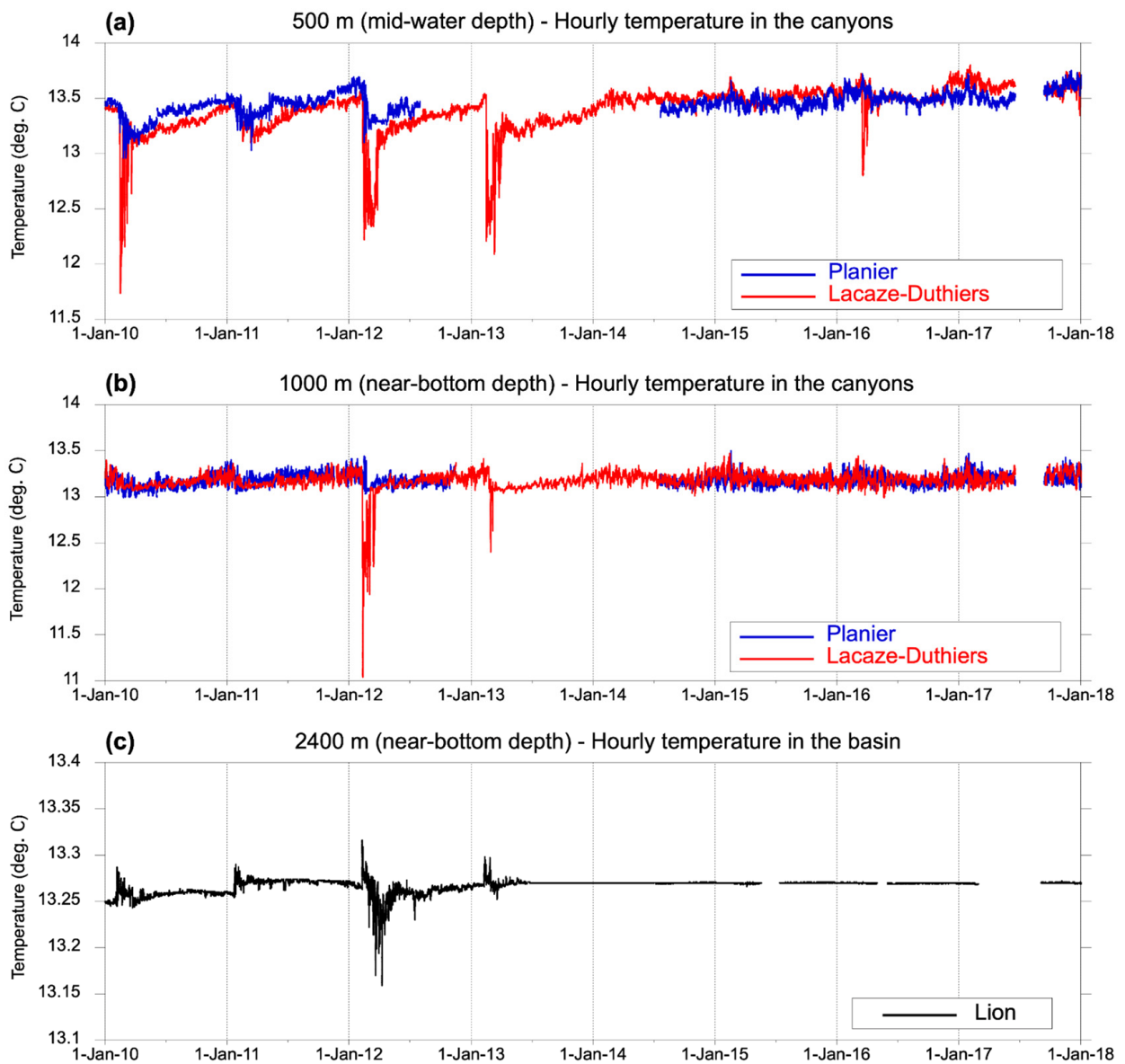


Figure 2. The 2010–2017 hourly time series of temperature (a) at 500 m deep (mid-water) in the Planier and Lacaze-Duthiers Canyons, (b) at 1000 m deep (near-bottom) in the Planier and Lacaze-Duthiers Canyons, and (c) at 2400 m deep (near bottom) in the basin at the Lions site. See Figure 1 for the location of the sites.

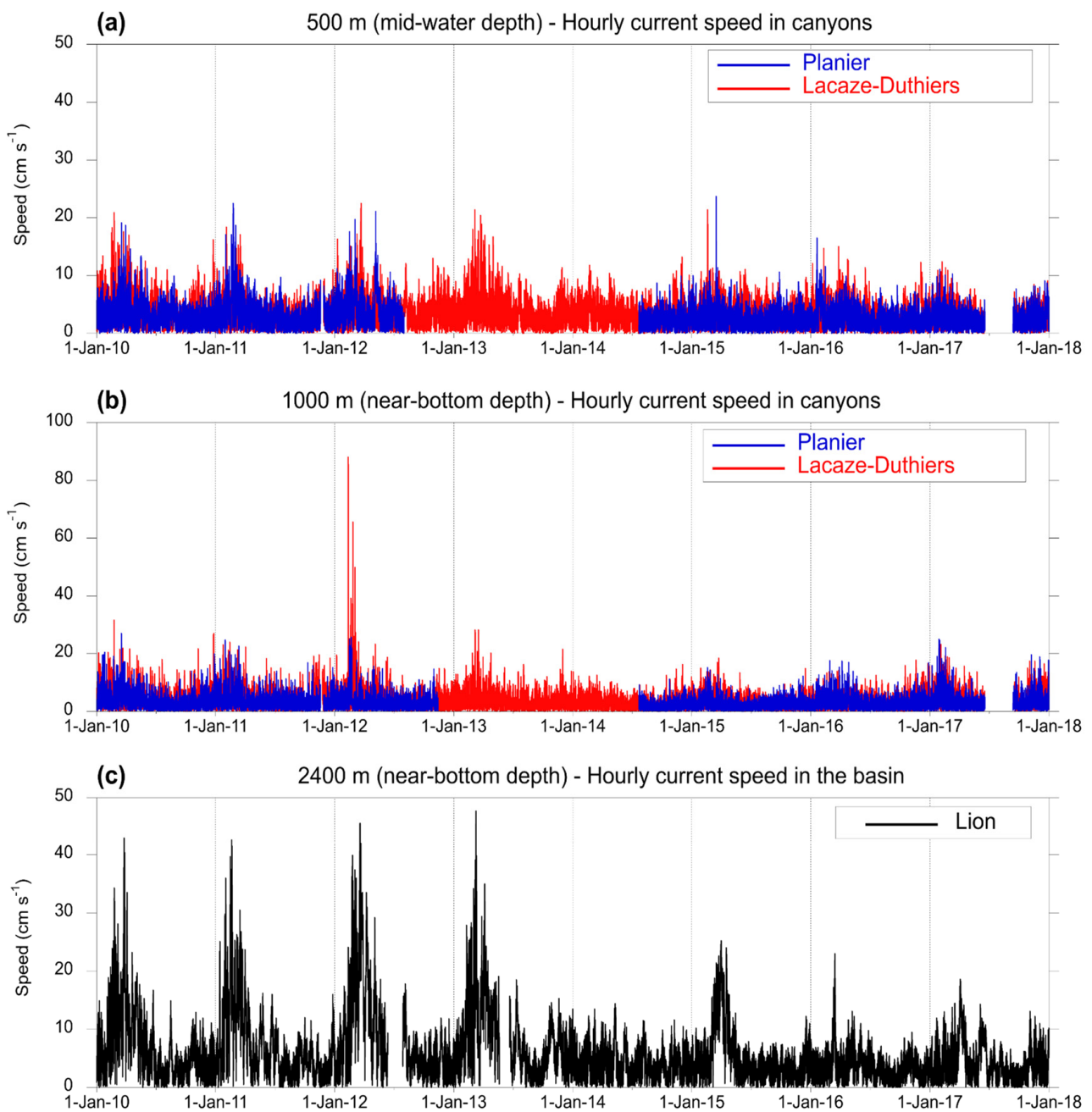


Figure 3. The 2010–2017 hourly time series of current speed (a) at 500 m deep (mid-water) in the Planier and Lacaze-Duthiers Canyons, (b) at 1000 m deep (near-bottom) in the Planier and Lacaze-Duthiers Canyons, (c) at 2400 m deep (near bottom) in the basin at the Lions site. See Figure 1 for the location of the sites.

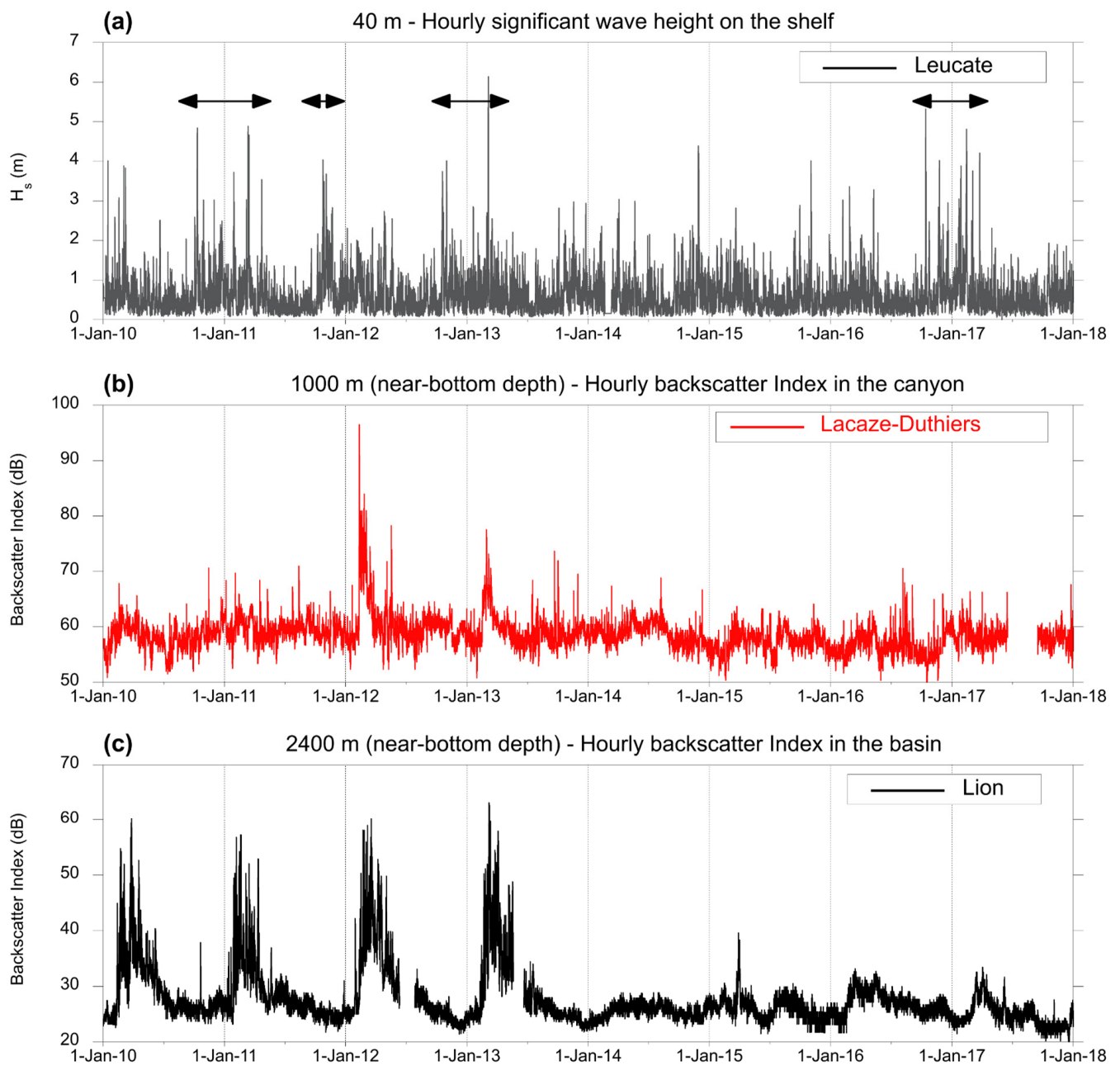


Figure 4. The 2010–2017 hourly time series of significant wave height at Leucate (a), backscatter index at 1000 m deep (near-bottom) in the Lacaze-Duthiers Canyon (b), and backscatter index at 2400 m deep (near-bottom) at the Lions site (c). Arrows indicate the period of the major S–SE storms. See Figure 1 for the location of the sites.

3.2. 2010–2017 Time Series of Particulate Fluxes

The 8-year records (2010–2017) of atmospheric, riverine, and oceanic particulate fluxes are presented in Figure 5.

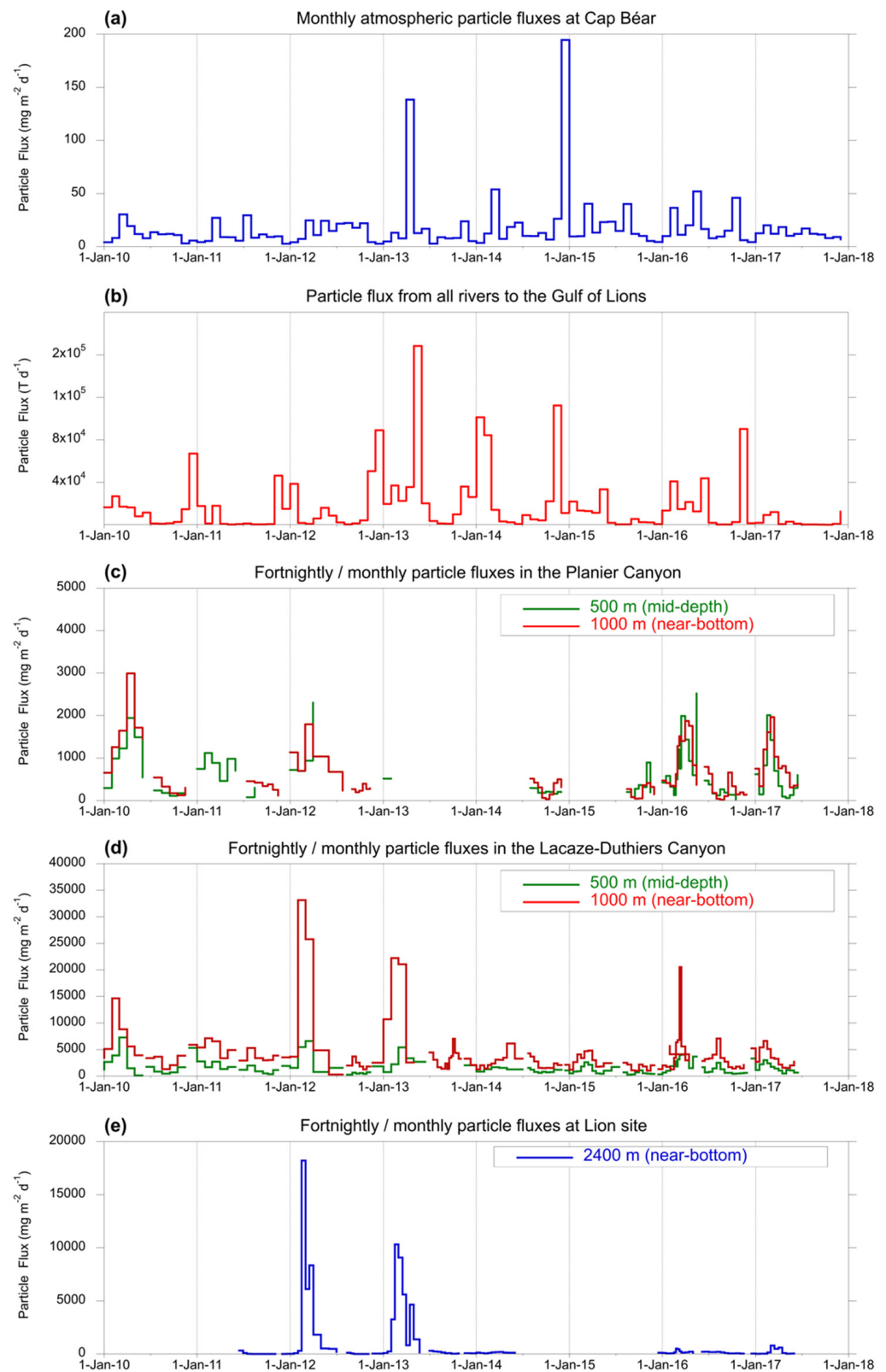


Figure 5. The 2010–2017 time series of the atmospheric, riverine, and oceanic particulate fluxes. (a) Atmospheric fluxes at Cap Béar; (b) aggregated river discharges; (c) particulate fluxes at 500 and 1000 m deep in the Planier Canyon; (d) particulate fluxes at 500 and 1000 m deep in the Lacaze-Duthiers Canyon; (e) particulate fluxes at 2400 m in the deep basin (Lions). Note the change in scale for the flux in the canyons and in the basin. See Figure 1 for the location of the sites.

The particulate atmospheric inputs are the sum of the dry fallout plus the particulate wet deposition. The monthly atmospheric fluxes measured at Cap Béar (Figure 5a) showed an average deposition around $17 \text{ mg/m}^2/\text{d}$ and a strong interannual variability with peaks up to $150\text{--}200 \text{ mg/m}^2/\text{d}$. However, they showed a seasonal variability with maximum fluxes between March and June and minimum fluxes in December–January.

The aggregate solid discharges of the rivers (Rhône, Hérault, Orb, Aude, Agly, and Têt; Figure 5b) were on average $1.7 \times 10^4 \text{ T/d}$ and showed a clear seasonal variability with maximum inputs around $1 \times 10^5 \text{ T/d}$ between November and February and minimum inputs around $1 \times 10^3 \text{ T/d}$ in August and September. The winters of 2013 to 2015 had the highest river discharges of the period 2010–2017. With 95% of the inputs, the Rhône largely predominated over the contribution of the other small coastal rivers.

Particle fluxes at 500 and 1000 m depth in the Planier Canyon (Figure 5c) showed a clear seasonal signal with maximum values during winter and were quite similar with an average of about $0.6 \times 10^3 \text{ mg/m}^2/\text{d}$.

Particle fluxes at a 500 m depth in the Lacaze-Duthiers Canyon (Figure 5d) were on average $1.6 \times 10^3 \text{ mg/m}^2/\text{d}$ with seasonal fluctuations characterized by increases of a factor of 2 in winter periods. Fluxes near the bottom at a 1000 m depth were systematically higher (average of $4.1 \times 10^3 \text{ mg/m}^2/\text{d}$) and were characterized by peaks during the winters of 2012 and 2013 with values between 2.2×10^4 and $3.3 \times 10^4 \text{ mg/m}^2/\text{d}$. Two other, shorter flux peaks appeared during the winters of 2010 and 2016; these events corresponded to the cascading detected at a 500 m but not at a 1000 m depth (Figure 5d)

Near-bottom fluxes in the convection zone (Figure 5e) had two periods with no measurements but captured the very large fluxes in the winters of 2012 and 2013 that peaked between 1×10^4 and $1.8 \times 10^4 \text{ mg/m}^2/\text{d}$. The rest of the time, the fluxes were low, around $80 \text{ mg/m}^2/\text{d}$.

3.3. Metals Concentrations during the 2011–2012 Period

Al-normalized metal concentrations were measured for all media (atmospheric deposition, riverine inputs, slope and basin particulate fluxes) only for the year 2012 (Figure 6). The results showed that the temporal variability of concentrations for the different metals were generally larger for sources (atmosphere and rivers) and deep basin fluxes than for canyon fluxes and for the superficial sediment. Sediments showed fairly similar concentrations regardless of where they were collected (shelf, slope or basin), and often showed the minimal lowest values across all media. The variability of metal contents in the Rhône River was lower than in other small coastal rivers and most of the elements, except Ni. In addition, the metal concentrations recorded in the Rhône particles were often close to those found in the sediments.

With only rare exceptions in the Planier Canyon at a 500 m depth, the concentrations for the particulate fluxes on the slope (PL500, PL1000, LD500, LD1000) and in the basin (LION) were minimal during the cascading and convection period (black star, Feb–Mar 2012). These were close to the average sediment value. Concentrations for all metals were lowest in the Lacaze-Duthiers Canyon (LD500, LD1000), where the dense shelf water cascading was the most intense.

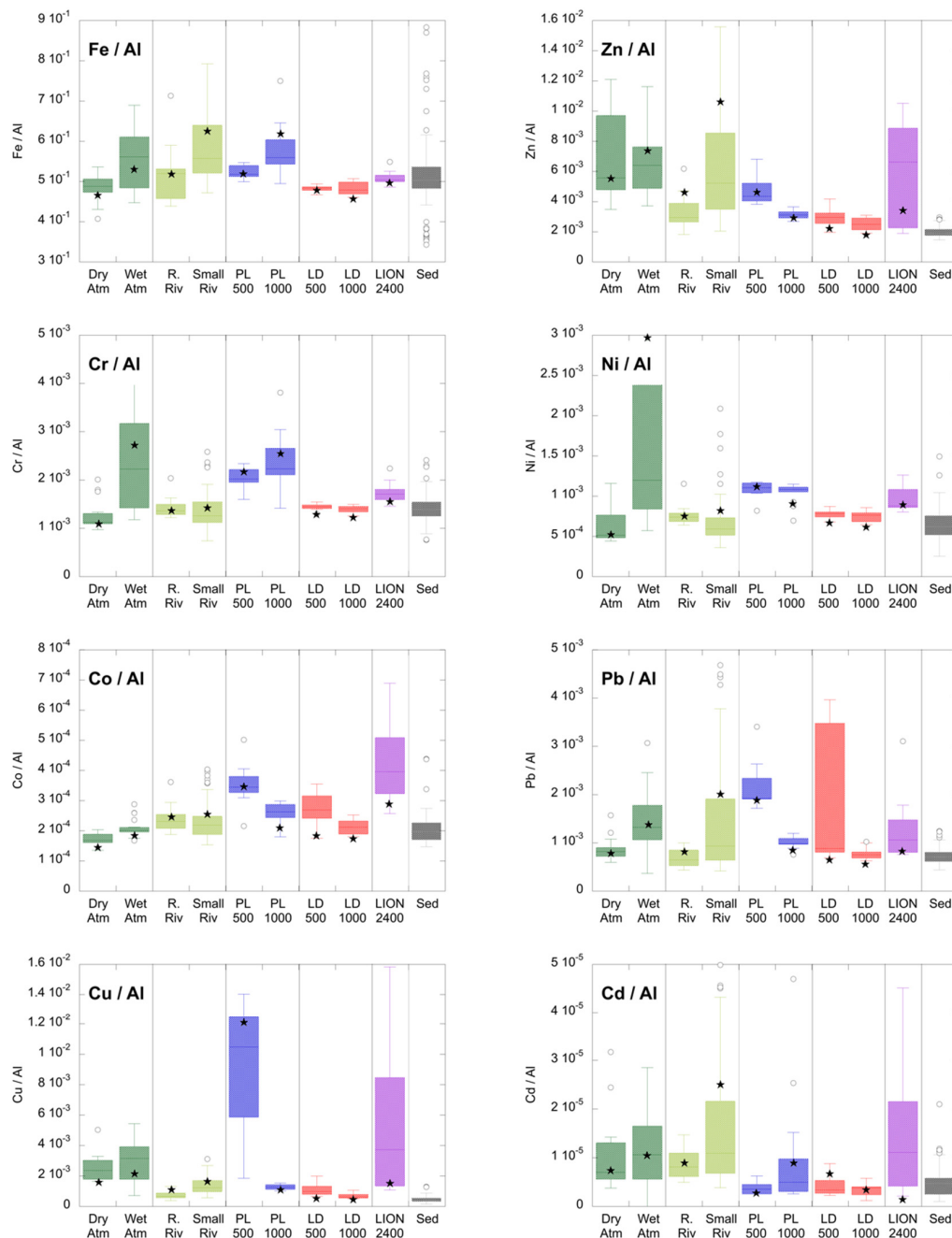


Figure 6. Box and whisker plots of selected Al-normalized metals (Zn, Cr, Ni, Co, Pb, Cu, Cd) for the particulate fluxes collected in dry (Dry Atm) and wet atmospheric (Wet Atm) deposits, in the Rhône River (R. Riv) and the other small rivers (Small Riv), in the Planier (PL) and Lacaze-Duthiers (LD) Canyons at 500 (mid-depth) and 1000 m (near-bottom), in the basin (LION) at 2400 m (near-bottom) as well as for the superficial sediments (Sed) measured for the year 2012. Average concentration for the cascading and convection events in February–March 2012 are indicated by black stars (★). See Figure 1 for the location of the sampled stations. Each box of the box and whisker plots encloses 50% (between the lower and upper quartiles) of the data with the median value of the variable displayed as a line. The length of the whiskers is restricted to a maximum of 1.5 times the interquartile range. Any value outside of this interval are represented as points and considered as potential outliers.

4. Discussion

4.1. Sediment Transport during Dense Water Formation Events

Several scenarios appeared in our dataset regarding their respective intensity (Figure 7). The winters of 2014 to 2017 exhibited low heat losses generating mixing limited to the surface layer, and dense water that formed at the coast or offshore sunk only to a few hundred meters of depth. The winters of 2010 and 2011 were characterized by intense convection, with mixing reaching the basin floor at 2400 m (which we will refer to as ‘deep convection events’), and cascading limited to a few hundred meters along the continental slope. The winters of 2012 and 2013 were characterized by deep convection and intense cascading (which we will call ‘deep cascading events’), all of which forms deep water that later mixes in the basin.

The effect of deep convection on sediment resuspension in the Gulf of Lions basin was suggested by [27] based on the first near-bottom particle trap measurements performed between 2007 and 2009. This effect was confirmed and detailed by [28]. These authors showed that during the winter of 2013, as convection reached the bottom, bottom currents larger than 25 cm/s were able to resuspend the surface sediments from the deep basin and generate a bottom nepheloid layer, with a maximum thickness of more than 2000 m, under the effect of strong vertical currents (up to 20 cm/s) present during the intense mixing phase. During the deep-water dispersion phase, which occurs when the convective mixing subsides and the water column restores itself, the bottom currents intensify up to 50 cm/s. They erode the deep sediments and transport them with the newly formed deep water within a bottom layer several hundred meters thick.

Deep cascading events also transport water and particulate matter from the coastal zone into the basin. The contribution of coastal waters to the formation of new deep waters was initially revealed by [43] following the intense dense water formation event of winter 1999. Its contribution was also shown during the massive events of 2005 and 2006, which led to a radical change in the characteristics of the deep waters of the western Mediterranean [44,45] as well as that of 2012 and 2013 [46]. Deep cascading events carry with them sedimentary material from the shelf and slope that they may have resuspended given their high velocities (Figures 3b and 4b). The erosive potential of dense water plumes on the shelf and in canyons has been observed by [24,47]. In [29], they showed that following the intense deep-water formation events of 1999 and 2005–2006, a positive turbidity anomaly (with concentrations < 0.1 mg/l above background levels) was associated with these new background waters and were visible throughout the western basin.

Together, these studies show that these new deep waters, resulting either from convection alone or from a combination of convection and cascading, could spread across the northwestern basin in a few months and occupy a large part of the western Mediterranean basin within a year. They allow for the dispersal of suspended particulate material from the resuspension of deep sediments of the Gulf of Lions, and possibly in the case of deep cascading, of sediment from the shelf and the continental slope.

Direct and indirect observations over the last 30 years of the cascading and convection events shown in Figure 8 illustrate the interannual variability of these two processes, with simultaneous intense events in 1999/2000, 2005/2006, and 2012/2013. A clear warming trend in the intermediate waters has appeared since 2014, which results from an accumulation of warm and salty Levantine intermediate waters following the weak intensity of winter convection. Incidentally, this evolution of intermediate waters increases the deep stratification that hinders the deepening of the mixed layer in winter due to air–sea heat losses. Climate simulations taking into account the most pessimistic scenarios (A2 for cascading [48] and RCP8.5 for convection [49,50] suggest that by the end of the 21st century, even from the middle of the century, increased stratification will be one of the main reasons for the significant decrease or even disappearance of deep cascading and convection events.

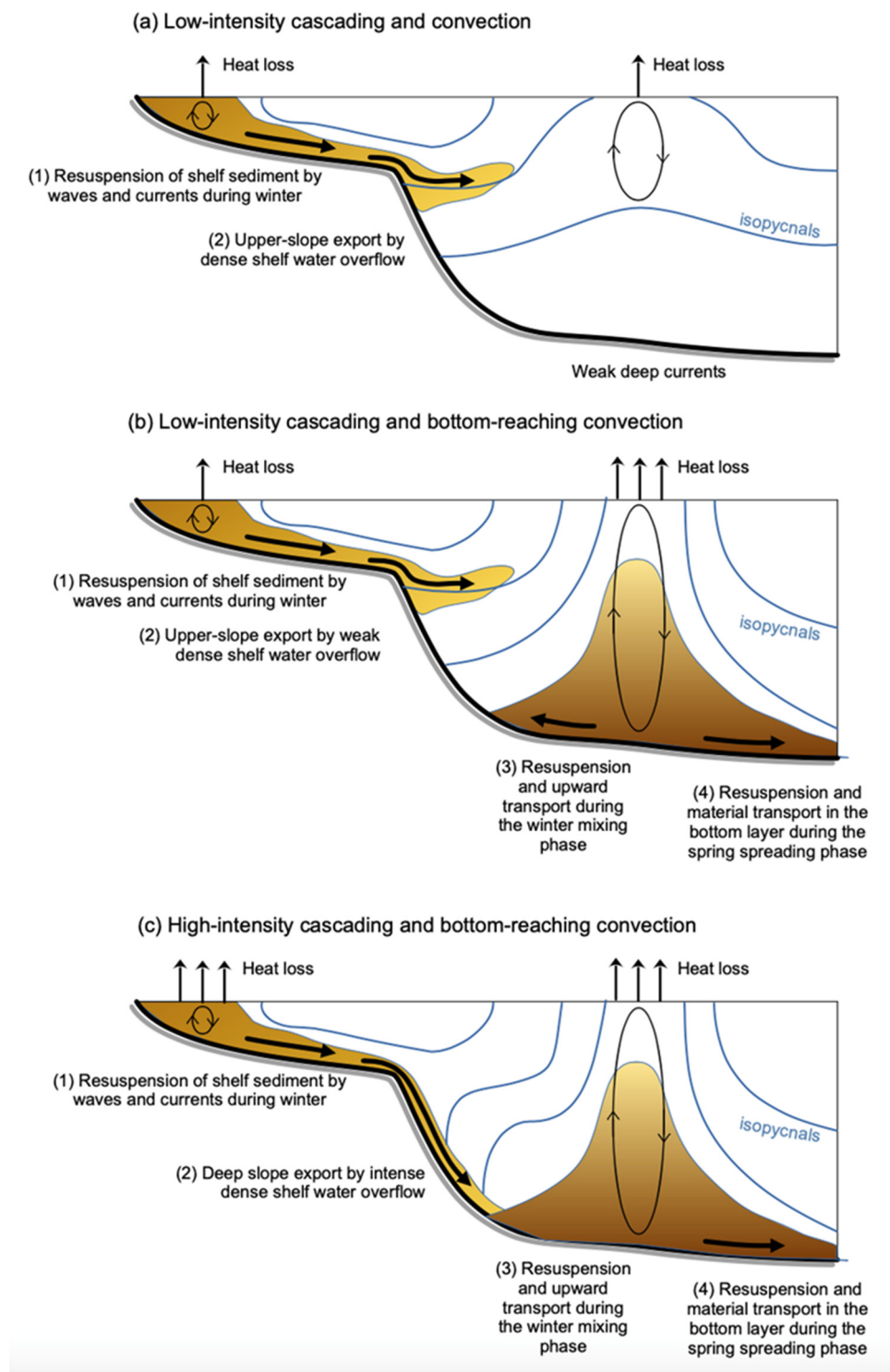


Figure 7. Sketches of the transport pathways of particulate fluxes from the coastal zone to the deep basin for different scenarios (a) during a severe winter event of dense shelf water cascading and bottom-reaching convection in the northwestern Mediterranean (winter 2012 and 2013 events), (b) during a severe E–SE storm (winter 2011), and (c) during a bottom-reaching convection only event. Black arrows to the atmosphere indicate heat loss, those in the water column indicate vertical mixing and lateral transport. Surfaces with the same density (isopycnals) are delineated by blue lines.

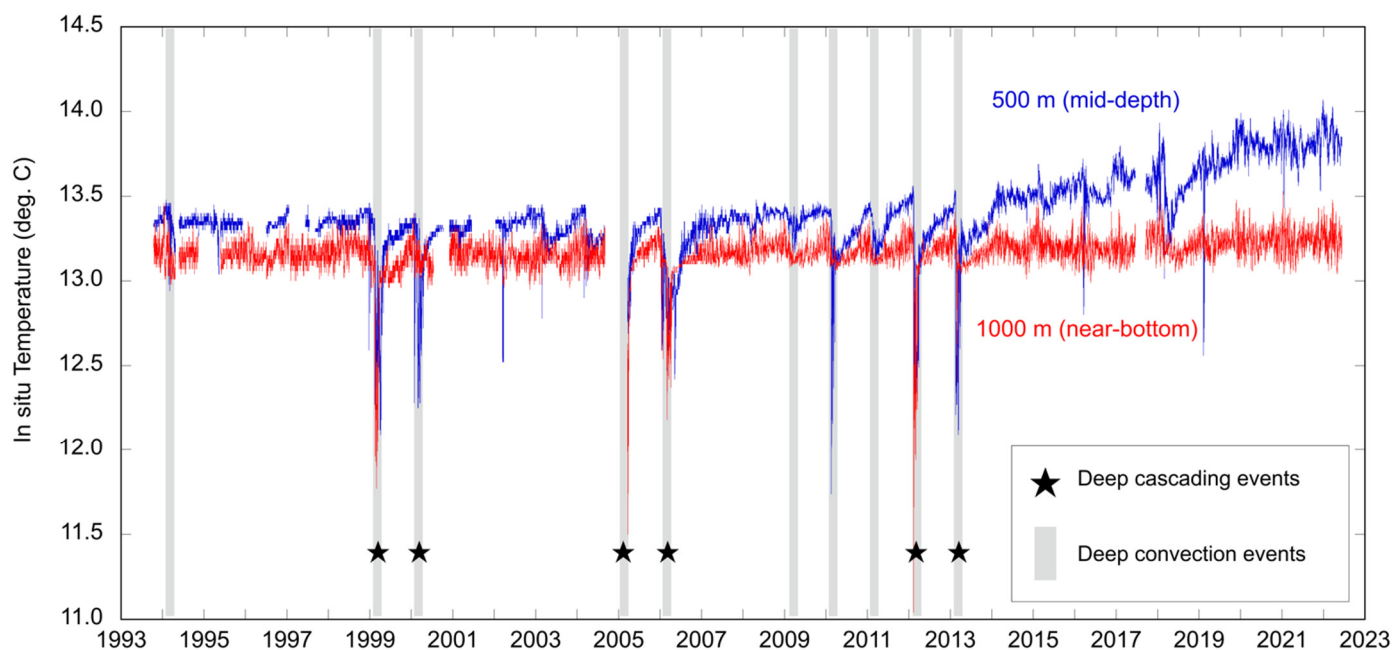


Figure 8. Temperature time series measured between October 1993 and June 2022 at 500 m and 1000 m depth in the Lacaze-Duthiers Canyon. Deep cascading events (after [22,24–26]) are indicated by black stars and deep convection events (after [43,45,46,51]) are indicated by grey bands.

The anticipated decrease in the intensity of export to the deep basin related to deep cascading events is likely to result in a change in the depositional areas of coastal sediments transported off the shelf. The sediments will be preferentially deposited at the edge of the shelf and along the upper continental slope.

4.2. Impact on the Fate of Metallic Elements in the Basin

Quantification for the year 2012 of the particulate and PTM inputs contributed by rivers and the atmosphere to the Gulf of Lions continental shelf as well as export from the shelf is presented in Table 1. The riverine inputs take into account the monthly measurements from different rivers in the Gulf of Lions. The atmospheric deposition considers the monthly measurements at the Cap Béar site extrapolated to the whole continental shelf of about 12,000 km² (from the coastline to the shelf break at 120 m deep). The fluxes exported from the continental shelf, delimited by the 100 m isobath, were based on estimates obtained by sediment transport modeling for the same period [52] and the mean January–March 2012 PTM concentrations measured at 1000 m deep in the Lacaze-Duthiers and Cap de Creus Canyons (Table 2).

Although the concentrations showed some variability (overall higher metal content in Lacaze-Duthiers particles), the normalization with respect to Al for each metal was very similar between the two canyons except for Cu and Cd, whose ratios were significantly lower in the particles collected at the outlet of the Cap de Creus Canyon. The lower concentrations in this canyon are certainly related to the granulometric effect. Indeed, the transfer of particles from the shelf to the Cap de Creus Canyon is carried out with much more energy, which allows for the transport of coarser particles with a lower metal content as well as less clay minerals able to adsorb anthropogenic metals such as Cu or Cd (Table 2).

In their study (see Figure 14 of [52]), the export of sediment from the shelf during the winter 2012 deep cascading event was estimated to about 1 Mt, which corresponds to about 15% of the total particulate load exported by rivers; the major part originating from the Rhône River (99%). Metal river fluxes recorded in 2012 are consistent with those previously reported by [18], who described two contrasting years (2001–2002) in terms of the water and particle discharge of the Rhône River (Table 1). Interestingly, the estimated proportions of

PTM in riverine fluxes exported by this cascading, except for Cd (39%), were quite similar (in the range 9–16%). Theoretically, Cd has a higher solubility and thus a preferential to be dissolved toward particulate phase exchange with increasing salinity [53] would be expected. However, Cd concentrations in the exported particles in the two canyons showed a significant difference (factor 20), which makes the conclusions more difficult for this element.

Table 1. Estimation of the riverine and atmospheric inputs of particulate matter and PMTs to the Gulf of Lions continental shelf for the entire year of 2012, and export from the shelf to the basin during winter 2012. The contribution of the Rhône and dry deposition to the total riverine and atmospheric deposition, respectively, is shown.

Element	Riverine Inputs (T) Rhône Contribution (%)	Atmospheric Deposition (T) Dry Contribution (%)	Atmospheric Deposition (This Study) (kg/km ²)	Atmospheric Deposition [51] (kg/km ²)	Cascading Offshelf Export (T)	Atmospheric/Riverine Input (%)	Cascading Offshelf Export/Riverine Input (%)	Cascading Offshelf Export/Atmospheric Input (%)
Particulate matter	6.7×10^6 (99%)	0.2×10^6 (73%)	16,667		$\sim 1 \times 10^6$	2.99	14.93	500
Al	3.8×10^5 (99%)	0.1×10^5 (63%)	833	144–918	0.57×10^5	2.63	15.01	570.5
Fe	2.0×10^5 (99%)	0.6×10^4 (61%)	500	840	0.28×10^5	3.00	14.05	468.3
Zn	1233 (98%)	68 (64%)	5.67	2	109.2	5.52	8.86	160.6
Cr	525 (99%)	19 (45%)	1.58	2.5	73.3	3.62	13.96	385.8
Ni	278 (99%)	10 (39%)	0.83	0.9	36.3	3.60	13.06	363.0
Co	84 (98%)	2 (62%)	0.17	0.05–0.4	10.6	2.38	12.62	530.0
Pb	238 (97%)	11 (50%)	0.92	3.2	37.5	4.62	15.76	340.9
Cu	233 (98%)	25 (67%)	2.08	2.7	29.2	10.73	12.53	116.8
Cd	3.8 (97%)	0.1 (49%)	0.008	0.31–1.3	1.5	2.63	39.47	1500

Table 2. PTM concentration in the Lacaze-Duthiers Canyon, Cap de Creus Canyon, and average concentration of the particulate matter at a 1000 m depth during the winter of 2012.

Element	Lacaze-Duthiers 1000 m (µg/g)	Cap de Creus 1000 m (µg/g)	Average Concentration (µg/g)
Al	66,247	47,855	57,051
Fe	30,534	25,663	28,099
Zn	126.3	92.1	109.2
Cr	83.1	63.4	73.3
Ni	42.6	29.9	36.3
Co	12.0	9.2	10.6
Pb	41.6	33.3	37.5
Cu	40.8	17.5	29.2
Cd	2.8	0.14	1.5

The estimate of the atmospheric particulate flux only represents 2.6% of the river fluxes (Table 1). The relative contribution of atmospheric fluxes to riverine metal fluxes varies from 2.6% (Al, Cd, Co) to 10.7% (Cu). This high value for Cu can be explained in the Cap Béar region (the dataset at this station was used as a reference to characterize at the best the atmospheric deposition all over the Gulf of Lions) by the widespread use of Cu as an antifungal agent in vineyards to counteract the effects of downy mildew.

Our atmospheric deposition data were in the same order of magnitude as those reported by [54] in the Gulf of Lions (Table 1). For all element fluxes, there was a large spatial and temporal variability across the NW Mediterranean Sea expressing both heterogeneous sources for trace metals and interannual atmospheric conditions (wet or dry year, wind conditions, particle load). Apparently, cascading is able to export about up to 5-fold the metallic atmospheric deposition (Al and Co), except for Cd for which, as explained earlier,

the calculations are less conclusive. It has been shown that for particulate riverine Cd, Cd in atmospheric aerosols is highly soluble in the range of 81–84% [55], explaining the low particulate cascading/atmospheric ratio.

Finally, the transport of particulate matter and PTMs from the shelf to the basin, essentially associated with the cascading event, represents between 8 and 15% of the total input (rivers and atmosphere). Thus, deep cascading events are likely to carry a notable proportion of the annual input of material and associated material to the deep basin.

The variability of metal concentrations in particulate fluxes in the basin reflects a mixture of sources, with higher concentrations likely to be associated with atmospheric inputs, and lower concentrations generally associated with sediment. Through remobilization of the shelf, slope, and basin sediment during extreme dense water formation events (albeit sporadic on a multi-decadal scale), it is therefore possible for locally derived continental particulate matter such as from the rivers of the Gulf of Lions to diffuse rapidly (on an annual scale) throughout the western Mediterranean Basin. These lateral inputs combine with inputs from atmospheric deposition that affect the entire surface of the western basin.

5. Conclusions

This study investigated the temporal variability of mass fluxes (rivers, atmosphere, slope, basin) during an 8-year period (2010–2017) in the Gulf of Lions (northwestern Mediterranean) collected under the MOOSE observatory. It clearly showed that intermittent events of dense shelf water cascading allowed for rapid and direct export from the shelf to the basin. If, simultaneously with this export, a deep convection event occurs, the particulate material is remobilized and dispersed over the entire western basin and contributes to deposition in the basin via lateral inputs that add to the sedimentation of atmospheric particulate material. This illustrates the combined effect of sediment transport processes associated with dense water formation processes that can cause the large-scale dispersion of local coastal inputs.

The decorrelation between the input events (primarily fluvial flooding) and output events (E–SE storms and cascading events) suggests that particulate matter accumulated on the shelf and slope may be exported years later. Therefore, it is necessary to work over the long-term (decadal) to integrate the different inflow and outflow events.

It appears that intense cascading events such as the 2012 event are likely to export to the deep basin a significant amount (about 15% for the 2012 year) of the annual input of continental particles and associated major metals that are primarily contributed by rivers.

Extreme deep cascading events will be less frequent with climate warming. This decrease will lead to a probable modification of the deposition areas, which should be limited to the upper slope.

Author Contributions: Conceptualization, X.D.d.M., D.A. and O.R.; Methodology, X.D.d.M., D.A., B.C. and S.K.; Analysis, X.D.d.M., B.C., C.M. and J.S.; Writing: X.D.d.M., D.A. and B.C. All authors have read and agreed to the published version of the manuscript.

Funding: This research was funded by the Mediterranean Ocean Observing System for the Environment (SNO-MOOSE of CNRS-INSU) and by the Hotspot Ecosystem Research and Man's Impact on European seas (HERMIONE FP7-ENV-2008-1) program.

Institutional Review Board Statement: Not applicable.

Informed Consent Statement: Not applicable.

Data Availability Statement: Original data used in this work are available through the MOOSE database (<http://mistrals.sedoo.fr/MOOSE/> (accessed on 21 November 2022)) and are referenced on SEANO (E) (<http://www.seano.org/data/00333/44411/> (accessed on 21 November 2022)); <http://www.seano.org/data/00349/45980/> (accessed on 21 November 2022)).

Acknowledgments: We acknowledge the support of ICM-CSIC and GRGM-UB for providing the results from the Cap de Creus Canyon. The authors acknowledge the three anonymous reviewers for their useful and constructive comments.

Conflicts of Interest: The authors declare no conflict of interest.

References

1. Katz, A.; Kaplan, I.R. Heavy Metals Behavior in Coastal Sediments of Southern California: A Critical Review and Synthesis. *Mar. Chem.* **1981**, *10*, 261–299. [\[CrossRef\]](#)
2. Bertolotto, R.M.; Tortarolo, B.; Frignani, M.; Bellucci, L.G.; Albanese, S.; Cuneo, C.; Alvarado-Aguilar, D.; Picca, M.R.; Gollo, E. Heavy Metals in Surficial Coastal Sediments of the Ligurian Sea. *Mar. Pollut. Bull.* **2005**, *50*, 348–356. [\[CrossRef\]](#) [\[PubMed\]](#)
3. Chandía, C.; Salamanca, M. Long-Term Monitoring of Heavy Metals in Chilean Coastal Sediments in the Eastern South Pacific Ocean. *Mar. Pollut. Bull.* **2012**, *64*, 2254–2260. [\[CrossRef\]](#)
4. Sharifuzzaman, S.M.; Rahman, H.; Ashekuzzaman, S.M.; Islam, M.M.; Chowdhury, S.R.; Hossain, M.S. Heavy Metals Accumulation in Coastal Sediments. In *Environmental Remediation Technologies for Metal-Contaminated Soils*; Hasegawa, H., Rahman, I.M.M., Rahman, M.A., Eds.; Springer: Tokyo, Japan, 2016; pp. 21–42. ISBN 978-4-431-55758-6.
5. García-Lorenzo, M.L.; Pérez-Sirvent, C.; Martínez-Sánchez, M.J.; Molina-Ruiz, J.; Martínez, S.; Arroyo, X.; Martínez-Martínez, L.B.; Bech, J. Potential Bioavailability Assessment and Distribution of Heavy Metal (Oids) in Cores from Portman Bay (SE, Spain). *GEEA* **2019**, *19*, 193–200. [\[CrossRef\]](#)
6. Ferré, B.; Durrieu de Madron, X.; Estournel, C.; Ulses, C.; Le Corre, G. Impact of Natural (Waves and Currents) and Anthropogenic (Trawl) Resuspension on the Export of Particulate Matter to the Open Ocean. *Cont. Shelf Res.* **2008**, *28*, 2071–2091. [\[CrossRef\]](#)
7. Ulses, C.; Estournel, C.; Durrieu de Madron, X.; Palanques, A. Suspended Sediment Transport in the Gulf of Lions (NW Mediterranean): Impact of Extreme Storms and Floods. *Cont. Shelf Res.* **2008**, *28*, 2048–2070. [\[CrossRef\]](#)
8. Palanques, A.; Puig, P.; Latasa, M.; Scharek, R. Deep Sediment Transport Induced by Storms and Dense Shelf-Water Cascading in the Northwestern Mediterranean Basin. *Deep Sea Res. Part I Oceanogr. Res. Pap.* **2009**, *56*, 425–434. [\[CrossRef\]](#)
9. Wright, L.D. Recent Advances in Understanding Continental Shelf Sediment Transport. In *Sediments, Morphology and Sedimentary Processes on Continental Shelves*; Li, M.Z., Sherwood, C.R., Hill, P.R., Eds.; John Wiley & Sons, Ltd.: Chichester, West Sussex, UK, 2013; pp. 159–172. ISBN 978-1-118-31117-2.
10. Colombo, M.; Li, J.; Rogalla, B.; Allen, S.E.; Maldonado, M.T. Particulate Trace Element Distributions along the Canadian Arctic GEOTRACES Section: Shelf-Water Interactions, Advective Transport and Contrasting Biological Production. *Geochim. Cosmochim. Acta* **2022**, *323*, 183–201. [\[CrossRef\]](#)
11. Durrieu de Madron, X.; Wiberg, P.L.; Puig, P. Sediment Dynamics in the Gulf of Lions: The Impact of Extreme Events. *Cont. Shelf Res.* **2008**, *28*, 1867–1876. [\[CrossRef\]](#)
12. Millot, C. The Gulf of Lions' Hydrodynamics. *Cont. Shelf Res.* **1990**, *10*, 885–894. [\[CrossRef\]](#)
13. Marshall, J.; Schott, F. Open-Ocean Convection: Observations, Theory and Models. *Rev. Geophys.* **1999**, *37*, 1–64. [\[CrossRef\]](#)
14. Roussiez, V.; Ludwig, W.; Probst, J.-L.; Monaco, A. Background Levels of Heavy Metals in Surficial Sediments of the Gulf of Lions (NW Mediterranean): An Approach Based on 133Cs Normalization and Lead Isotope Measurements. *Environ. Pollut.* **2005**, *138*, 167–177. [\[CrossRef\]](#)
15. Roussiez, V.; Ludwig, W.; Monaco, A.; Probst, J.-L.; Bouloubassi, I.; Buscail, R.; Saragoni, G. Sources and Sinks of Sediment-Bound Contaminants in the Gulf of Lions (NW Mediterranean Sea): A Multi-Tracer Approach. *Cont. Shelf Res.* **2006**, *26*, 1843–1857. [\[CrossRef\]](#)
16. Roussiez, V.; Heussner, S.; Ludwig, W.; Radakovitch, O.; Durrieu de Madron, X.; Guieu, C.; Probst, J.-L.; Monaco, A.; Delsaut, N. Impact of Oceanic Floods on Particulate Metal Inputs to Coastal and Deep-Sea Environments: A Case Study in the NW Mediterranean Sea. *Cont. Shelf Res.* **2012**, *45*, 15–26. [\[CrossRef\]](#)
17. Radakovitch, O.; Roussiez, V.; Ollivier, P.; Ludwig, W.; Grenz, C.; Probst, J.-L. Input of Particulate Heavy Metals from Rivers and Associated Sedimentary Deposits on the Gulf of Lion Continental Shelf. *Estuar. Coast. Shelf Sci.* **2008**, *77*, 285–295. [\[CrossRef\]](#)
18. Ollivier, P.; Radakovitch, O.; Hamelin, B. Major and Trace Element Partition and Fluxes in the Rhône River. *Chem. Geol.* **2011**, *285*, 15–31. [\[CrossRef\]](#)
19. Dumas, C.; Ludwig, W.; Aubert, D.; Eyrolle, F.; Raimbault, P.; Gueneugues, A.; Sotin, C. Riverine Transfer of Anthropogenic and Natural Trace Metals to the Gulf of Lions (NW Mediterranean Sea). *Appl. Geochem.* **2015**, *58*, 14–25. [\[CrossRef\]](#)
20. Grousset, F.E.; Quétel, C.R.; Thomas, B.; Donard, O.F.X.; Lambert, C.E.; Guillard, F.; Monaco, A. Anthropogenic vs. Lithogenic Origins of Trace Elements (As, Cd, Pb, Rb, Sb, Sc, Sn, Zn) in Water Column Particles: Northwestern Mediterranean Sea. *Mar. Chem.* **1995**, *48*, 291–310. [\[CrossRef\]](#)
21. Dumas, C.; Aubert, D.; Durrieu de Madron, X.; Ludwig, W.; Heussner, S.; Delsaut, N.; Menniti, C.; Sotin, C.; Buscail, R. Storm-Induced Transfer of Particulate Trace Metals to the Deep-Sea in the Gulf of Lion (NW Mediterranean Sea). *Environ. Geochem. Health* **2014**, *36*, 995–1014. [\[CrossRef\]](#) [\[PubMed\]](#)
22. Heussner, S.; Durrieu de Madron, X.; Calafat, A.; Canals, M.; Carbonne, J.; Delsaut, N.; Saragoni, G. Spatial and Temporal Variability of Downward Particle Fluxes on a Continental Slope: Lessons from an 8-Yr Experiment in the Gulf of Lions (NW Mediterranean). *Mar. Geol.* **2006**, *234*, 63–92. [\[CrossRef\]](#)
23. Palanques, A.; Durrieu de Madron, X.; Puig, P.; Fabres, J.; Guillén, J.; Calafat, A.; Canals, M.; Heussner, S.; Bonnín, J. Suspended Sediment Fluxes and Transport Processes in the Gulf of Lions Submarine Canyons. The Role of Storms and Dense Water Cascading. *Mar. Geol.* **2006**, *234*, 43–61. [\[CrossRef\]](#)

24. Canals, M.; Puig, P.; de Madron, X.D.; Heussner, S.; Palanques, A.; Fabres, J. Flushing Submarine Canyons. *Nature* **2006**, *444*, 354–357. [[CrossRef](#)] [[PubMed](#)]
25. Palanques, A.; Puig, P.; Durrieu de Madron, X.; Sanchez-Vidal, A.; Pasqual, C.; Martín, J.; Calafat, A.; Heussner, S.; Canals, M. Sediment Transport to the Deep Canyons and Open-Slope of the Western Gulf of Lions during the 2006 Intense Cascading and Open-Sea Convection Period. *Prog. Oceanogr.* **2012**, *106*, 1–15. [[CrossRef](#)]
26. Durrieu de Madron, X.; Houpert, L.; Puig, P.; Sanchez-Vidal, A.; Testor, P.; Bosse, A.; Estournel, C.; Somot, S.; Bourrin, F.; Bouin, M.N.; et al. Interaction of Dense Shelf Water Cascading and Open-Sea Convection in the Northwestern Mediterranean during Winter 2012. *Geophys. Res. Lett.* **2013**, *40*, 1379–1385. [[CrossRef](#)]
27. Stabholz, M.; Durrieu de Madron, X.; Canals, M.; Khrifounoff, A.; Taupier-Letage, I.; Testor, P.; Heussner, S.; Kerhervé, P.; Delsaut, N.; Houpert, L.; et al. Impact of Open-Ocean Convection on Particle Fluxes and Sediment Dynamics in the Deep Margin of the Gulf of Lions. *Biogeosciences* **2013**, *10*, 1097–1116. [[CrossRef](#)]
28. Durrieu de Madron, X.; Ramondenc, S.; Berline, L.; Houpert, L.; Bosse, A.; Martini, S.; Guidi, L.; Conan, P.; Curtil, C.; Delsaut, N.; et al. Deep Sediment Resuspension and Thick Nepheloid Layer Generation by Open-Ocean Convection. *J. Geophys. Res. Ocean.* **2017**, *122*, 2291–2318. [[CrossRef](#)]
29. Puig, P.; Durrieu de Madron, X.; Salat, J.; Schroeder, K.; Martín, J.; Karageorgis, A.P.; Palanques, A.; Roullier, F.; Lopez-Jurado, J.L.; Emelianov, M.; et al. Thick Bottom Nepheloid Layers in the Western Mediterranean Generated by Deep Dense Shelf Water Cascading. *Prog. Oceanogr.* **2013**, *111*, 1–23. [[CrossRef](#)]
30. Palanques, A.; Puig, P. Particle Fluxes Induced by Benthic Storms during the 2012 Dense Shelf Water Cascading and Open Sea Convection Period in the Northwestern Mediterranean Basin. *Mar. Geol.* **2018**, *406*, 119–131. [[CrossRef](#)]
31. Guerzoni, S.; Molinaroli, E.; Chester, R. Saharan Dust Inputs to the Western Mediterranean Sea: Depositional Patterns, Geochemistry and Sedimentological Implications. *Deep Sea Res. Part II Top. Stud. Oceanogr.* **1997**, *44*, 631–654. [[CrossRef](#)]
32. Vincent, J.; Laurent, B.; Losno, R.; Bon Nguyen, E.; Rouillet, P.; Sauvage, S.; Chevaillier, S.; Coddeville, P.; Ouboulmane, N.; di Sarra, A.G.; et al. Variability of Mineral Dust Deposition in the Western Mediterranean Basin and South-East of France. *Atmos. Chem. Phys.* **2016**, *16*, 8749–8766. [[CrossRef](#)]
33. Sadaoui, M.; Ludwig, W.; Bourrin, F.; Raimbault, P. Controls, Budgets and Variability of Riverine Sediment Fluxes to the Gulf of Lions (NW Mediterranean Sea). *J. Hydrol.* **2016**, *540*, 1002–1015. [[CrossRef](#)]
34. Heussner, S.; Ratti, C.; Carbonne, J. The PPS 3 Time-Series Sediment Trap and the Trap Sample Processing Techniques Used during the ECOMARGE Experiment. *Cont. Shelf Res.* **1990**, *10*, 943–958. [[CrossRef](#)]
35. Testor, P.; Durrieu De Madron, X.; Mortier, L.; D’ortenzio, F.; Legoff, H.; Dausse, D.; Labaste, M.; Houpert, L. LION Observatory Data; SEANO. 2020. Available online: <http://www.seano.org/data/00333/44411/> (accessed on 21 November 2022).
36. Arnaud, M. *REMORA3 Cruise*; L’Europe R/V, Ifremer: Plouzané, France, 2002. [[CrossRef](#)]
37. Durrieu de Madron, X. *DEEP/4 Cruise*; L’Europe R/V, Ifremer: Plouzané, France, 2009. [[CrossRef](#)]
38. Durrieu de Madron, X. *CASCADE Cruise*; L’Atalante R/V, Ifremer: Plouzané, France, 2011. [[CrossRef](#)]
39. Durrieu de Madron, X.; Stabholz, M.; Heimbürger-Boavida, L.-E.; Aubert, D.; Kerhervé, P.; Ludwig, W. Approaches to Evaluate Spatial and Temporal Variability of Deep Marine Sediment Characteristics under the Impact of Dense Water Formation Events. *Medit. Mar. Sci.* **2020**, *21*, 527–544. [[CrossRef](#)]
40. Lohrmann, A. Monitoring Sediment Concentration with Acoustic Backscattering Instruments. *Nortek Tech. Note* **2001**, *3*, 1–5. Available online: <https://www.nortekgroup.com/assets/documents/Monitoring-sediment-concentration-with-acoustic-backscattering-instruments.pdf> (accessed on 10 January 2023).
41. Guillén, J.; Bourrin, F.; Palanques, A.; Durrieu de Madron, X.; Puig, P.; Buscail, R. Sediment Dynamics during Wet and Dry Storm Events on the Têt Inner Shelf (SW Gulf of Lions). *Mar. Geol.* **2006**, *234*, 129–142. [[CrossRef](#)]
42. Dufois, F.; Garreau, P.; Le Hir, P.; Forget, P. Wave- and Current-Induced Bottom Shear Stress Distribution in the Gulf of Lions. *Cont. Shelf Res.* **2008**, *28*, 1920–1934. [[CrossRef](#)]
43. Bethoux, J.P.; Durrieu de Madron, X.; Nyffeler, F.; Tailliez, D. Deep Water in the Western Mediterranean: Peculiar 1999 and 2000 Characteristics, Shelf Formation Hypothesis, Variability since 1970 and Geochemical Inferences. *J. Mar. Syst.* **2002**, *33–34*, 117–131. [[CrossRef](#)]
44. Font, J.; Puig, P.; Salat, J.; Palanques, A.; Emelianov, M. Sequence of Hydrographic Changes in NW Mediterranean Deep Water Due to the Exceptional Winter of 2005. *Sci. Mar.* **2007**, *71*, 339–346. [[CrossRef](#)]
45. Schroeder, K.; Ribotti, A.; Borghini, M.; Sorgente, R.; Perilli, A.; Gasparini, G.P. An Extensive Western Mediterranean Deep Water Renewal between 2004 and 2006. *Geophys. Res. Lett.* **2008**, *35*, L18605. [[CrossRef](#)]
46. Houpert, L.; Durrieu de Madron, X.; Testor, P.; Bosse, A.; D’Ortenzio, F.; Bouin, M.N.; Dausse, D.; Le Goff, H.; Kunesch, S.; Labaste, M.; et al. Observations of Open-Ocean Deep Convection in the Northwestern Mediterranean Sea: Seasonal and Interannual Variability of Mixing and Deep Water Masses for the 2007–2013 Period: DEEP CONVECTION OBS. NWMED 2007–2013. *J. Geophys. Res. Ocean.* **2016**, *121*, 8139–8171. [[CrossRef](#)]
47. Bourrin, F.; Durrieu de Madron, X.; Heussner, S.; Estournel, C. Impact of Winter Dense Water Formation on Shelf Sediment Erosion (Evidence from the Gulf of Lions, NW Mediterranean). *Cont. Shelf Res.* **2008**, *28*, 1984–1999. [[CrossRef](#)]
48. Herrmann, M.; Estournel, C.; Déqué, M.; Marsaleix, P.; Sevault, F.; Somot, S. Dense Water Formation in the Gulf of Lions Shelf: Impact of Atmospheric Interannual Variability and Climate Change. *Cont. Shelf Res.* **2008**, *28*, 2092–2112. [[CrossRef](#)]

49. Soto-Navarro, J.; Jordá, G.; Amores, A.; Cabos, W.; Somot, S.; Sevault, F.; Macías, D.; Djurdjevic, V.; Sannino, G.; Li, L.; et al. Evolution of Mediterranean Sea Water Properties under Climate Change Scenarios in the Med-CORDEX Ensemble. *Clim. Dyn.* **2020**, *54*, 2135–2165. [[CrossRef](#)]
50. Parras-Berrocal, I.M.; Vázquez, R.; Cabos, W.; Sein, D.V.; Álvarez, O.; Bruno, M.; Izquierdo, A. Surface and Intermediate Water Changes Triggering the Future Collapse of Deep Water Formation in the North Western Mediterranean. *Geophys. Res. Lett.* **2022**, *49*, e2021GL095404. [[CrossRef](#)]
51. Margirier, F.; Testor, P.; Heslop, E.; Mallil, K.; Bosse, A.; Houpert, L.; Mortier, L.; Bouin, M.-N.; Coppola, L.; D’Ortenzio, F.; et al. Abrupt Warming and Salinification of Intermediate Waters Interplays with Decline of Deep Convection in the Northwestern Mediterranean Sea. *Sci. Rep.* **2020**, *10*, 20923. [[CrossRef](#)]
52. Estournel, C.; Mikolajczak, G.; Ulses, C.; Bourrin, F.; Canals, M.; Charmasson, S.; Doxaran, D.; Duhaut, T.; de Madron, X.D.; Marsaleix, P.; et al. Sediment Dynamics in the Gulf of Lion (NW Mediterranean Sea) during Two Autumn–Winter Periods with Contrasting Meteorological Conditions. *Prog. Oceanogr.* **2023**, *210*, 102942. [[CrossRef](#)]
53. Kraepiel, A.M.L.; Chiffolleau, J.-F.; Martin, J.-M.; Morel, F.M.M. Geochemistry of Trace Metals in the Gironde Estuary. *Geochim. Cosmochim. Acta* **1997**, *61*, 1421–1436. [[CrossRef](#)]
54. Guieu, C.; Loÿe-Pilot, M.-D.; Benyahya, L.; Dufour, A. Spatial Variability of Atmospheric Fluxes of Metals (Al, Fe, Cd, Zn and Pb) and Phosphorus over the Whole Mediterranean from a One-Year Monitoring Experiment: Biogeochemical Implications. *Mar. Chem.* **2010**, *120*, 164–178. [[CrossRef](#)]
55. Hodge, V.; Johnson, S.R.; Goldberg, E.D. Influence of Atmospherically Transported Aerosols on Surface Ocean Water Composition. *Geochem. J.* **1978**, *12*, 7–20. [[CrossRef](#)]

Disclaimer/Publisher’s Note: The statements, opinions and data contained in all publications are solely those of the individual author(s) and contributor(s) and not of MDPI and/or the editor(s). MDPI and/or the editor(s) disclaim responsibility for any injury to people or property resulting from any ideas, methods, instructions or products referred to in the content.